

2D Turbulent Jets on Rough and Smooth Boundaries

Shazy Shabayek

Department of Irrigation and Hydraulics, Faculty of Engineering, Ain Shams University, Cairo, Egypt
Corresponding Author: Shazy Shabayek

Abstract: This paper presents an experimental study on wall jets on rough and smooth boundaries with shallow tailwater depth. The main objective was to study the effect of the wall roughness on the characteristics of plane turbulent wall jets. Ten experiments in 3 sets were performed. Series A, consisting of four experiments, was performed on a smooth boundary; Series B, consisting of 3 experiments, was performed on a rough boundary with relative roughness of 0.212; Series C, consisting of 3 experiments, was performed on a rougher boundary with relative roughness of 0.379. The tailwater depth and the head gate opening were kept constant throughout the ten experiments. Froude number ranged between 3.8 and 8.0. The time averaged velocity profiles at different x-stations along the longitudinal direction of the flume, the bed shear stress, the water surface profile and the length of the surface eddy were measured in all the experiments. It was found that the velocity similarity profiles deviated from those for the classical wall jet and this deviation increased with relative roughness. The length of the surface eddy and the normalized shear stress were found to decrease with the increase in relative roughness. However, the decay of the max velocity, the growth of the jet half width, and the variation of the jet discharge and the jet momentum with distance were all found to be independent of the Froude number and the relative roughness.

Date of Submission: 25-03-2018

Date of acceptance: 09-04-2018

I. Introduction

The topic of submerged wall jets has been the focus of many researchers. This is due to their engineering application in energy dissipation downstream of hydraulic structures including drop structures, spillways, barrages and weirs. The submerged jumps can be considered as a transitional phenomenon between wall jets and free jumps (Kishore and Dey 2016). An earlier study by the author (Shabayek 2007) showed that the flow could be identified as a submerged jump or a wall jet based on the normalized velocity profiles. The study concluded that for the range of the Froude numbers and the Reynolds numbers used in the present study, the flow could be classified as a wall jet not a submerged jump (Shabayek 2007).

Consider a plane turbulent wall jet with a flow rate per unit width, Q_0 and momentum flux per unit width, M_0 , entering a rectangular channel tangentially on its bed as shown in Fig. 1. Let b_0 and U_0 be the thickness and the velocity of the jet at the slot, respectively. As soon as the jet issues from the slot, a re-circulating flow region starts to develop above the jet as shown in Fig. 1b. The length of this re-circulating region is referred to as the eddy length L_e . It is approximately the distance from the gate, housing the slot, to the section at which the jet surfaces. The experiments showed a depression in the water surface elevation at the gate, δ_w , with respect to the tailwater surface elevation. Förthmann (1936) carried an experimental study on plane turbulent wall-jets that showed that the axial velocity at any x-station, u , increased from zero at the wall to a maximum value, u_m , at a distance $y=\delta$ and then decreased to reach zero as shown in Fig. 1c. If b is the distance above the bed at which the velocity is $0.5u_m$ and $\partial u/\partial y$ is negative, the study concluded that the mean velocity field develops in a self similar manner, that the half-width, b , grows linearly, and that the u_m is inversely proportional to the square root of the distance from the slot.

For turbulent wall jets discharged into vast ambient of the same fluid (classical wall jets) it was generally assumed that the jet momentum flux is preserved (Albertson et al. 1950, Rajaratnam 1976 and Schlichting 1979). In 2002, Ead and Rajaratnam studied plane turbulent wall jets in shallow tailwater. The tailwater depth ratio $\eta=y_t/b_0$ (where y_t is the tailwater depth) ranged from 25 to 50. They found that the momentum flux in the forward flow region of the wall jet was not preserved. This was attributed to the rise in the water surface at the end of the surface eddy as well as the entrainment of the return flow. They hypothesized that a depression in the water surface at the gate was created to produce the pressure gradient required to drive the return flow above the wall jet to be entrained by the jet. In 2004, Ead and Rajaratnam conducted another experimental study on wall jets on rough boundaries with limited tailwater depth. They concluded that "The axial velocity profiles at the different sections in the wall jet were similar with some difference from the profile of the classical plane wall jet." It was also concluded that "the normalized boundary layer thickness δ/b was equal to 0.35 compared to 0.16 for the classic wall jet." The decay of the maximum velocity and the growth of

the length scale (which was defined as the longitudinal distance from the slot to where $u_m=0.5 U_o$) were found to occur in two stages; the first, near the slot, corresponded to the decay of the deep tailwater depth and in the second stage, the decay occurred at a faster rate due to the shallow tailwater.

In all these previous studies, different tailwater depth ratios were examined to check for a limiting value that could be considered as a shallow tailwater depth. Furthermore, the effect of the boundary roughness, for different shallow tailwater depth ratios, on the decay of the maximum velocity was studied. This study presents the results of an experimental investigation of plane turbulent wall jets with finite tailwater depth. Three series of experiments were performed; series A with smooth boundary, series B with relative boundary roughness of 0.212, and series C with relative boundary roughness of 0.379. The tailwater depth ratio was equal to 20 in all experiments. This was done to study the effect of the boundary roughness on the growth of the wall jet, the decay of the maximum velocity, the variation of the momentum and volume fluxes in the forward flow region and the shear stress on the bed, for a shallow tailwater depth condition.

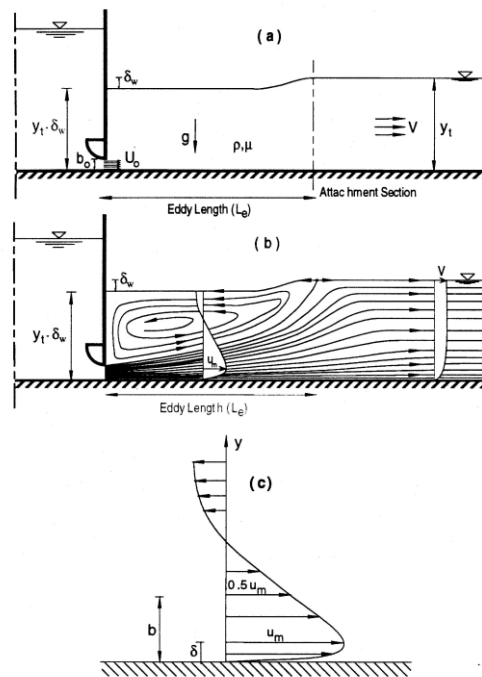


Fig. 1 Plane turbulent wall jet (a) Definition sketch; (b) Flow pattern; (c) Typical velocity distribution (Ead 1999)

II. Experimental Setup and Experiments

The experiments were performed in a re-circulating flume, 0.15 m wide, 0.3 m deep and 2.45m long, with plexiglass sides. The bed was adjusted to be horizontal in all the experimental runs. A single-leaf gate with a streamlined lip was used to produce a supercritical stream with a thickness equal to the gate opening b_o . At the downstream end of the flume, a tailgate was installed to control the tailwater depth. A metal tank, located under the flume, was used to collect the outflow and a centrifugal pump discharged it back into the flume. The bed of the flume was made of steel sheets covered with plastic sheets to give the smooth surface. False floors, with the same width of the flume, were used to create the rough bed. These false floors were made by fixing uniformly distributed sand grains, to the plastic sheets, using an adhesive water resistant material. A Prandtl tube, fit on a carriage that moved in the longitudinal and transverse directions was used to measure the time averaged velocity, u , at different x -stations along the longitudinal direction of the flume. The Prandtl tube was connected to a manometer board fixed on the side wall of the flume. The Prandtl tube was also used as a Preston tube for measuring the shear stress (Preston 1954 and Patel 1965). All the measurements were taken in the middle third of the flume.

Three sets of experiments, with 10 runs, were conducted. The primary details of these experiments are shown in Table 1. In series A, the experiments were performed on smooth bed. In series B and C, the experiments were performed on a rough bed with relative roughness, t/b_o , of 0.212 and 0.379, respectively, where t was the thickness of roughness. In all the runs, the gate opening was equal to 1 cm, the tailwater depth ratio η was equal to 20, and the Froude number was in the range of 3.8-8.0. The Reynolds number was in the range of 12400-25200. In all the experiments, the drop of the water surface elevation at the gate, δ_w , from that of

the tailwater as well as the length of the surface eddy, L_e , were measured. The length of the surface eddy was found by dye injection.

Table 1 Primary Details of Experiments

Expt.	b_o (cm)	t/b_o	U_o (m/s)	F_o	η	R_n
A-1	1.0	0.000	2.26	7.2	20.0	22600
A-2	1.0	0.000	1.88	6.0	20.0	18800
A-3	1.0	0.000	2.52	8.0	20.0	25200
A-4	1.0	0.000	1.24	4.0	20.0	12400
B-1	1.0	0.212	2.12	6.8	20.0	21200
B-2	1.0	0.212	1.87	6.0	20.0	18700
B-3	1.0	0.212	1.24	4.0	20.0	12400
C-1	1.0	0.379	2.26	7.2	20.0	22600
C-2	1.0	0.379	1.85	5.9	20.0	18500
C-3	1.0	0.379	1.20	3.8	20.0	12000

III. Results and Analysis:

Fig. 2 shows typical velocity profiles along with the water surface profiles for wall jets, on smooth and rough beds, for experiments A-1, B-1 and C-1. The figure shows the velocity profiles in the forward as well as the reverse flow at several sections with x/b_o ranging between 8 and 100, where x is the longitudinal distance from the gate housing the slot. In Fig. 2, y is the vertical distance above the bed. It can be observed from the figure that the water surface in the vicinity of the gate is horizontal. The water surface elevation then decreases in the flow direction until it reaches a minimum and then it increases further downstream. The rise can be seen to occur in the region where x is between 60 and 100 cm. This is the region in which the jet surfaces. The depression in the water surface elevation at the gate, δ_w , is also shown in the figure. The shear layer that separates the forward and backward flows is distinct in all the experiments. However no velocity measurements could be taken in that layer. The maximum reverse velocity for any experiment was found to occur at a distance of about $L_e/2$ from the gate. A comparison between the velocity profiles of the three experiments, presented in Fig. 2, indicates the effect of roughness. It can be seen that maximum forward flow velocity as well as the eddy length decrease with roughness.

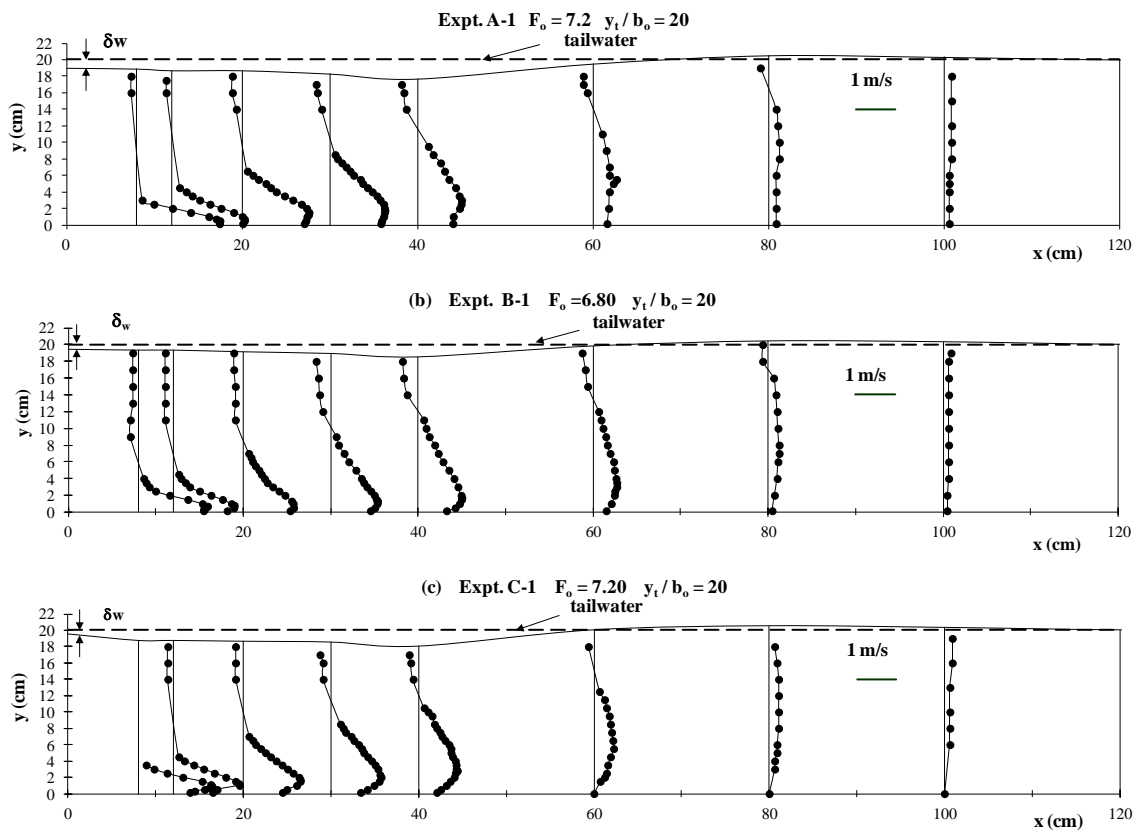


Fig. 2 Typical Velocity Profiles for Experiments (a) A-1 (b) B-1 (c) C-1

Considering the length of the surface eddy, L_e , it can be written that:

$$L_e = f[U_o, b_o, t, g, \nu, y_t] \tag{1}$$

Where ν is the kinematic viscosity.

Using the Pi theorem it can be shown that:

$$\frac{L_e}{b_o} = f_1\left[\frac{y_t}{b_o}, \frac{U_o}{\sqrt{gb_o}}, \frac{t}{b_o}, \frac{U_o b_o}{\nu}\right] \tag{2}$$

For large values of the Reynolds number viscous effects may be neglected and equation (2) reduces to:

$$\frac{L_e}{b_o} = f_1\left[\eta, F_o, \frac{t}{b_o}\right] \tag{3}$$

Since the tailwater depth ratio, η , was kept constant in this study, the effect of the relative boundary roughness, t/b_o and the Froude number at the slot, F_o , on the eddy length could be studied. Fig. 3 shows the variation of the normalized eddy length L_e/b_o with F_o for the three series of experiments. The figure shows that the eddy length increases with the increase in F_o . Furthermore, it can be seen that as the relative roughness increases the eddy length decreases and the jet surfaces closer to the gate. This can be attributed to the increase in the bed shear force, opposing the jet flow, with the increase in roughness.

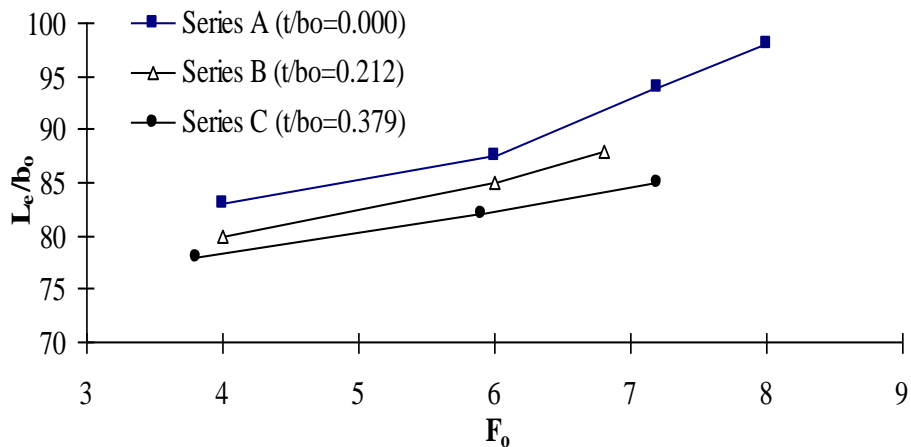


Fig. 3 The variation of the normalized eddy length L_e/b_o with F_o

The maximum velocity u_m and the distance b are considered as the velocity scale and the length scale, respectively, that are used to check for the similarity of the velocity profiles. Figs. 4(a, b and c) present typical velocity profiles at different x stations for experiment A-2, on smooth bed, experiment B-2, on rough bed with relative roughness $t/b_o=0.212$ and experiment C-2, on rough bed with relative roughness $t/b_o=0.379$ respectively. The normalized velocity profiles for the same experiments are presented in Figs. 4(d, e, and f). The velocity profiles are found to be similar. However, the similarity profile deviated from that of the classical wall jet. This deviation is possibly due to the interaction between the forward flow and the backward flow, the effect of the shallowness, the effect of the non horizontal water surface profile and the wavy surface. It can be seen from Figs. 4(d, e, and f) that the deviation from the classical wall jet increased with roughness. Fig. 5 shows a consolidated plot for all the data for each series. Figs. 5(a, b, and c) show the plot for all the experiments in series A, B, and C, respectively. Fig. 5 confirms the deviation of the velocity profiles from the classical wall jet with the increase in the relative roughness. Furthermore, the thickness of the boundary layer, δ , was found to be 0.24 times b_o for series A, 0.29 times b_o for series B and 0.36 times b_o for series C whereas δ is about 0.18 times b_o in the classical wall jet. It is concluded that the relative boundary layer thickness increases with roughness.

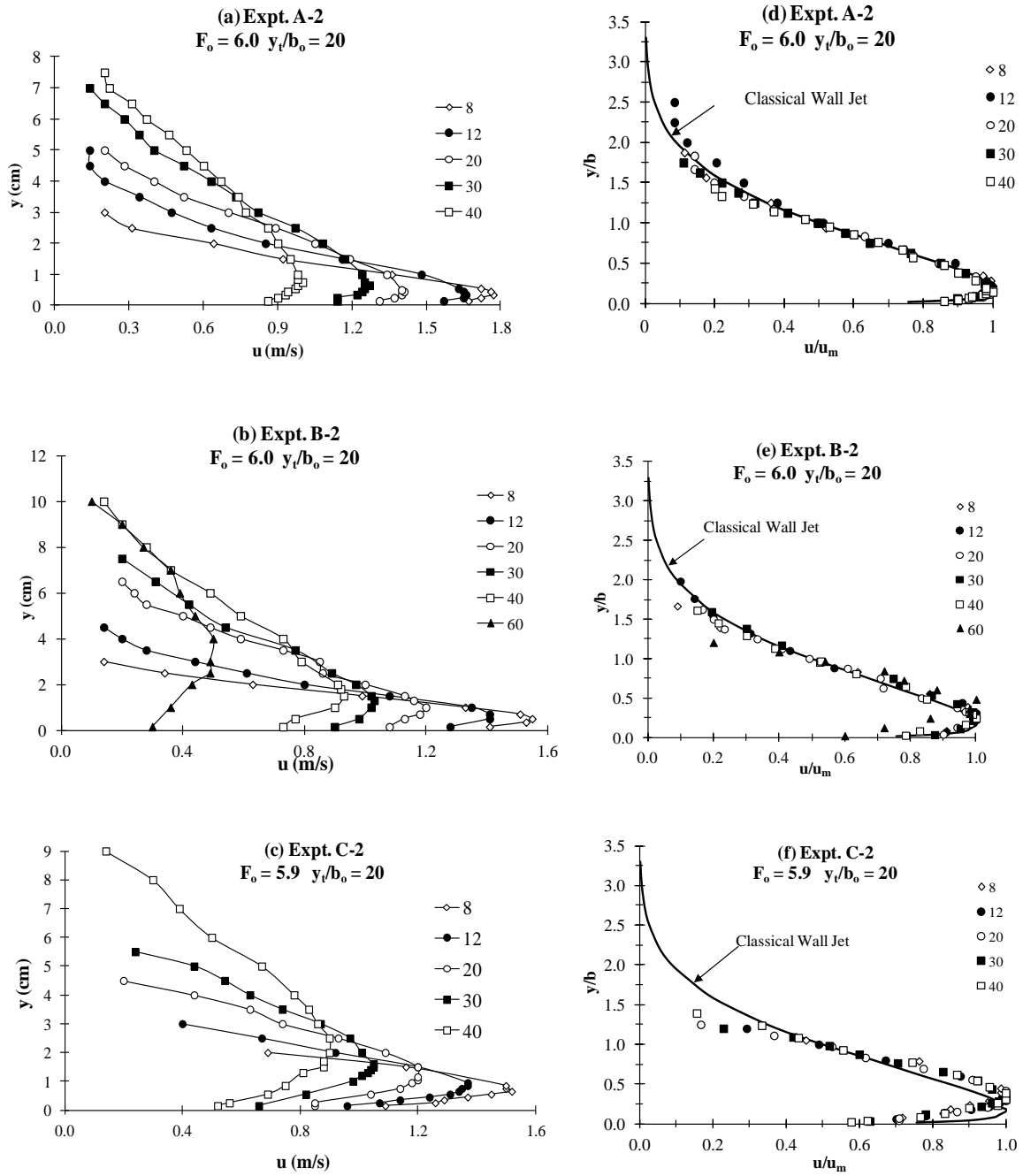


Fig. 4 Velocity distribution (a), (b) and (c) Velocity Profiles (d), (e) and (f) Similarity Profiles (For Experiments A-2, B-2 and C-2)

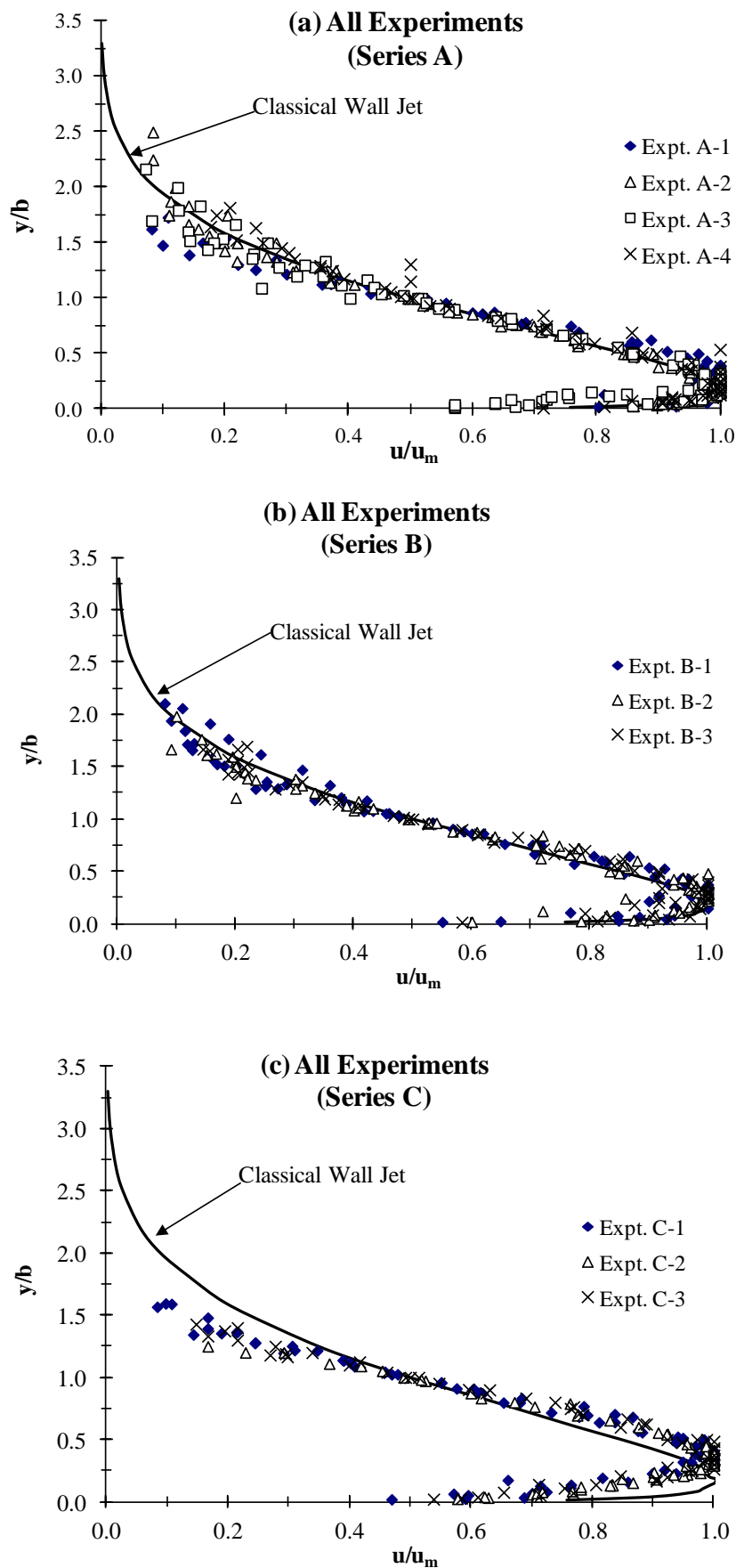


Fig. 5 Consolidated non dimensional plot for the velocity distribution in the wall jet.

To study the variation of the velocity scale, u_m , and the length scale, b , with the distance x , L was used to normalize the distance x , where L is defined as the value of x where $u_m=U_o/2$. (Wu and Rajaratnam 1995) showed that:

$$\frac{u_m}{U_o} = \frac{C}{\sqrt{x/L}} \tag{4}$$

for the classical wall jet where C is a constant equal to 0.5. They also found out that L/b_o is approximately equal to 60 for deep tailwater depth. Fig. 6 shows the decay of the maximum velocity, u_m , at any section in terms of the velocity of the jet at the slot, U_o , with the normalized distance, x/L . The decay of the maximum velocity for the classical wall jet is also presented in the figure. The figure shows that the decay of the maximum velocity happens in two stages similar to the findings of (Ead and Rajaratnam 2004). In the first stage the decay of the maximum velocity follows approximately that for the classical wall jet. This occurs up to a section at which the effect of the shallow tailwater depth is sensed by the jet. This initiates a faster decay for the maximum velocity and indicates the second stage. The figure also shows that the Froude number and the boundary roughness have no significant effect on the velocity decay. "The advantage of using L as the length scale is that the constant C in Eq. (4) is equal to 0.5 for both smooth and rough boundaries." (Ead and Rajaratnam 2004) Fig. 7 shows the variation of L/b_o with F_o . It can be seen from the figure that L/b_o is independent of the Froude number, F_o , and the relative roughness, t/b_o . A value of $L/b_o=39.8$ was deduced from the data for the range of F_o and t/b_o used in this study.

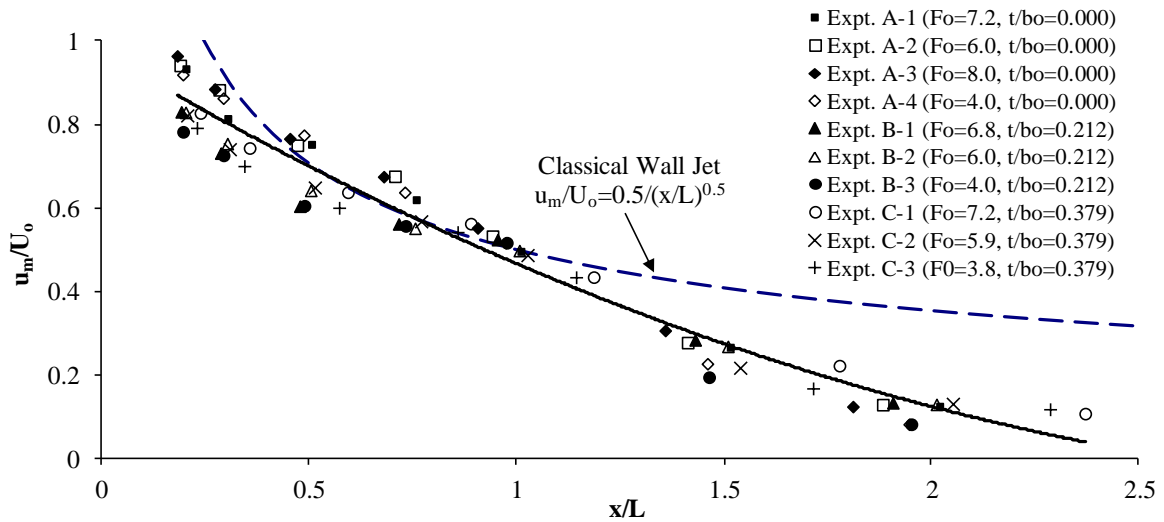


Fig. 6 Variation of the maximum velocity with distance

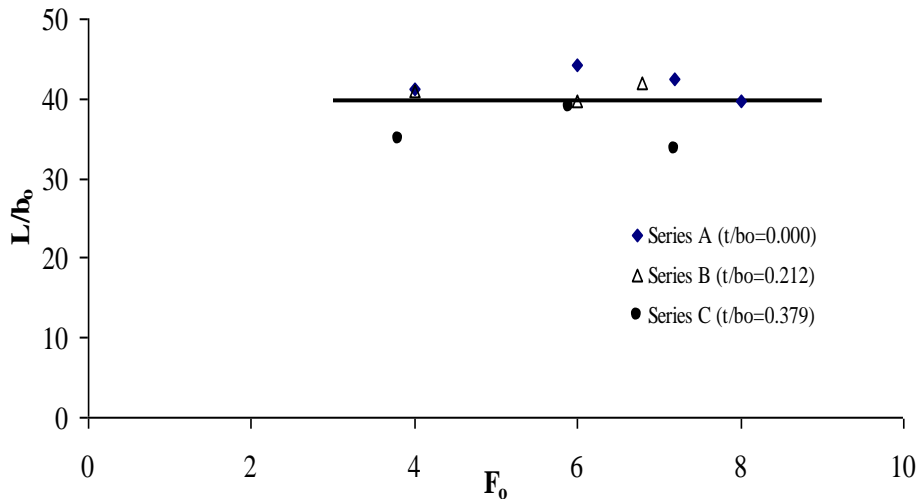


Fig. 7 The variation of the length scale ratio, L/b_o with F_o for all experiments

Fig. 8 shows the growth of the length scale b (or the jet half-width) with distance. The growth rate of

the classical wall jet (0.068) is also shown in the figure. The growth rate was 0.16 up to a certain section after which the growth rate became 0.4. The value of 0.16 is larger than the value of 0.125 found by Ead and Rajaratnam (2004) for wall jets on rough boundaries with limited tailwater. This may be attributed to using a rougher boundary with $t/b_o=0.379$ compared to $t/b_o=0.25$ used by Ead and Rajaratnam (2004). The change in the growth rate occurred at x/b_o of about 60 which is the section at which the effect of the shallow tailwater sets in. The figure shows that the growth rate is independent of the Froude number F_o and the boundary roughness for their ranges used in this study.

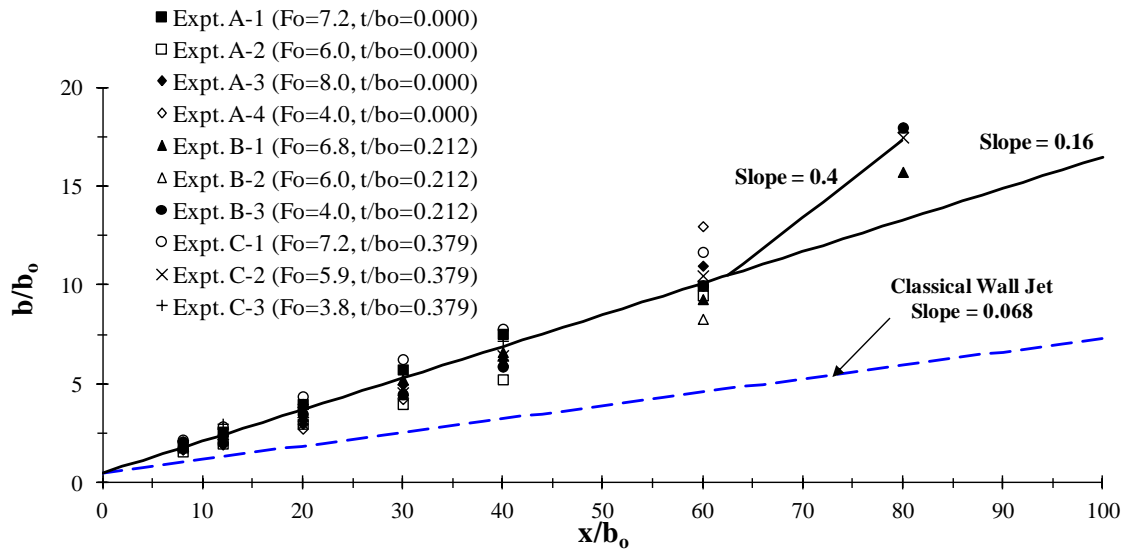


Fig. 8 The variation of the scale b (jet half-width) with distance

The velocity measurements at every section in each experiment were used to calculate the forward flow rate, Q , and the forward momentum flux, M , per unit width. Fig. 9 shows the variation of the relative discharge Q/Q_o (where Q_o is the discharge at the slot) with the normalized distance x/b_o . For the classical wall jet with a large value of η , the variation of Q/Q_o with x/b_o should be independent of the tailwater depth ratio and for this jet Q/Q_o would be proportional to $(x/b_o)^{0.5}$. This equation is presented in Fig. 9 with the value of the proportionality coefficient in this relation equal to 0.35. The figure shows that the relative discharge increases with the normalized distance at a rate greater than that of the classical wall jet up to a certain section and then decreases rapidly until it eventually reaches the value of 1. This is attributed to the shallow tailwater depth (Shabayek 2011). However, there is no significant effect for the Froude number, F_o , or the relative roughness on this variation. The variation of Q/Q_o with x/b_o is described by a cubic equation in the form:

$$\frac{Q}{Q_o} = A' \left(\frac{x}{b_o} \right)^3 + B' \left(\frac{x}{b_o} \right)^2 + C' \left(\frac{x}{b_o} \right) + 1 \tag{5}$$

where A' , B' and C' are functions of the tailwater depth ratio (Ead and Rajaratnam 2002). Ead (1999) found that the longitudinal distance at which the discharge reached a maximum, x_{Qm} , decreased with the decrease in the tailwater depth ratio. Ead (1999) found that $x_{Qm}/b_o=140$ for $\eta=50$ and decreased to $x_{Qm}/b_o =65$ for $\eta=25$. Fig. 9 shows that $x_{Qm}/b_o =35$ for the $\eta=20$ used in this study.

It was mentioned above that when the tailwater depth is relatively shallow, the wall jet could lose a substantial amount of the momentum flux of the forward flow as it travels downstream. This loss was attributed to the negative momentum carried by the entrained fluid which approached the fluid at an angle of $\pi/4$ radians from the forward direction of the jet (Kostovinos 1978). Fig. 10 shows the variation of the normalized momentum flux of the jet with the normalized distance. The figure shows that the momentum flux variation is similar to that of the mass flow rate where the normalized momentum flux increases up to a certain section after which it starts to decay. This can be due to the fact that the momentum flux is proportional to the product of the mass flow rate and the jet velocity. The mass flow rate varies with distance through a cubic equation, Eq. (5) while the maximum velocity decays (in the near field) with distance x through a power equation in the order of 0.5 similar to Eq. (4). This causes the mass flow rate variation to affect the momentum flux more significantly than the velocity and results in the similar variation of the momentum flux with distance to that of the jet discharge. The average loss in the momentum flux reaches a value of 90%. This can be attributed to the depression in the water surface at the gate δ_w . This depression causes an adverse pressure gradient that opposes the forward flow. The figure shows that the variation of the forward momentum flux with x/b_o is independent of

F_o and the relative roughness

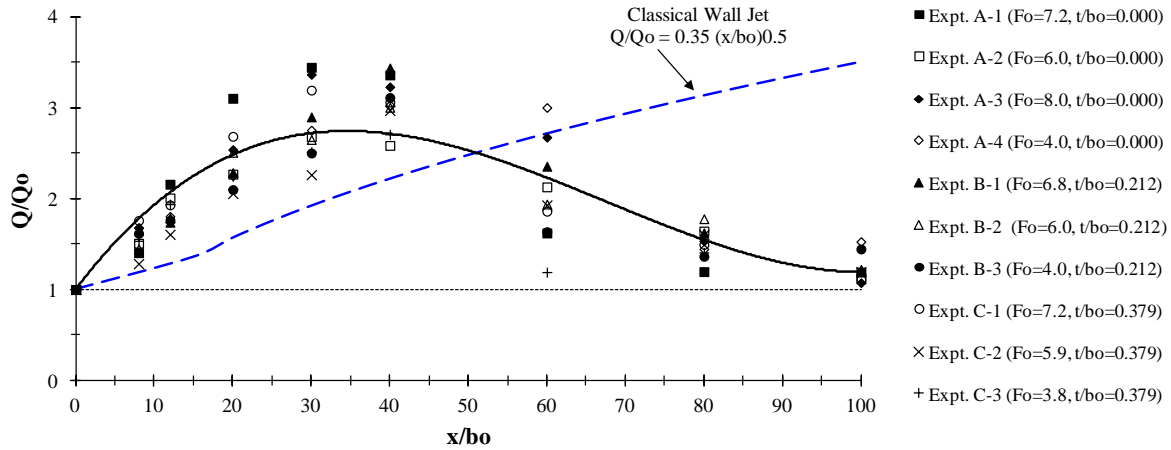


Fig. 9 Variation of the wall jet discharge with distance

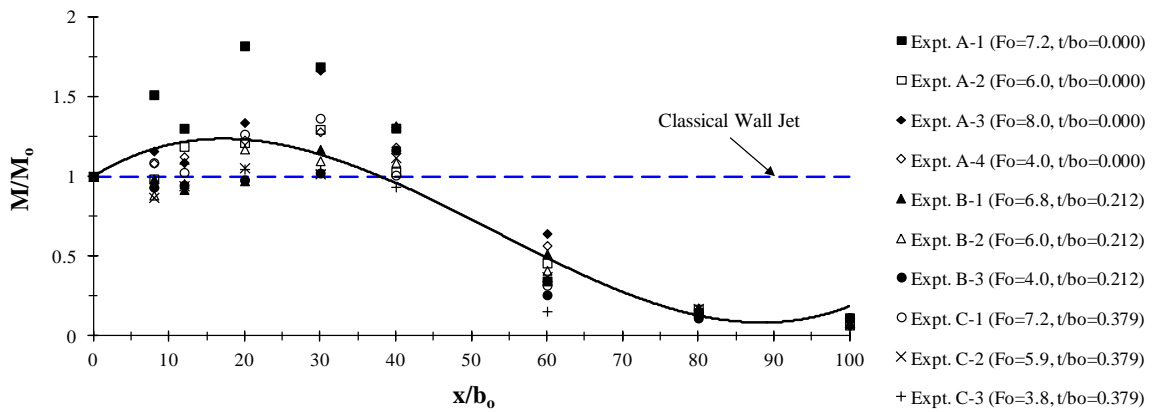


Fig. 10 The variation of the jet momentum with distance.

Fig. 11 presents the variation of the depression ratio, $\theta = \delta_w/b_o$, with the Froude number. The figure shows that θ increases with the increase in the Froude number and this increase is more profound for the smooth boundary (Series A) than for the rough ones (Series B and C). Furthermore, the figure indicates that the depression ratio decreases with the increase in the relative roughness.

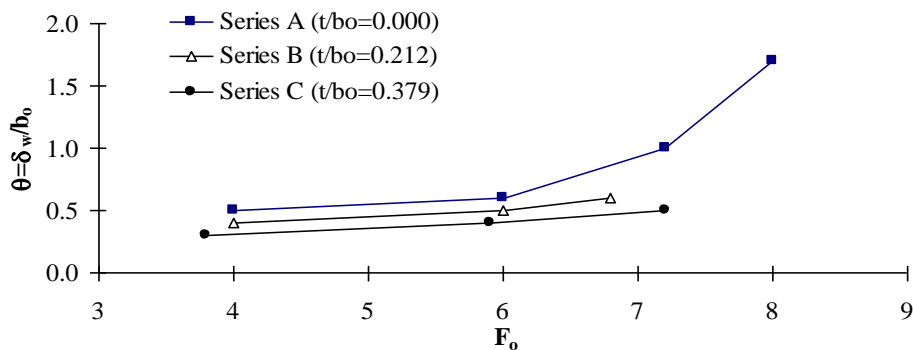


Fig. 11 The variation of the depression ratio δ_w/b_o with the Froude number F_o

The integrated shear stress was experimentally evaluated in this study as it is one of the primary forces involved in the momentum equation. Figs. 12 (a, b, and c) present the variation of the bed shear stress with distance for Series A, Series B and Series C, respectively. The figure shows that the shear stress increases with the increase in Reynolds number. Fig. 13 presents the variation of normalized shear stress with the normalized

distance where the maximum shear stress, τ_m is chosen as the shear scale. Fig. 13 shows that the profiles are similar for each series and the normalized shear stress decreases with distance. Furthermore, the normalized shear stress decreases with the increase in relative roughness for a certain x/b_o . The influence of the Reynolds number on the chosen shear scale τ_m is presented in Fig. 14. The maximum shear stress increases linearly with Reynolds number. Fig. 15 presents the variation of the shear force coefficient $\epsilon_x = F_{\tau x} / M_o$ with x/b_o where ϵ_x and $F_{\tau x}$ are the shear force coefficient and the integrated bed shear stress at a longitudinal distance x from the slot, respectively. It can be seen that ϵ_x increases with x/b_o . The figure confirms the results obtained from figure 14 where the profiles are similar for each series and the values of the shear force coefficient at a certain distance decrease as the relative roughness values increase.

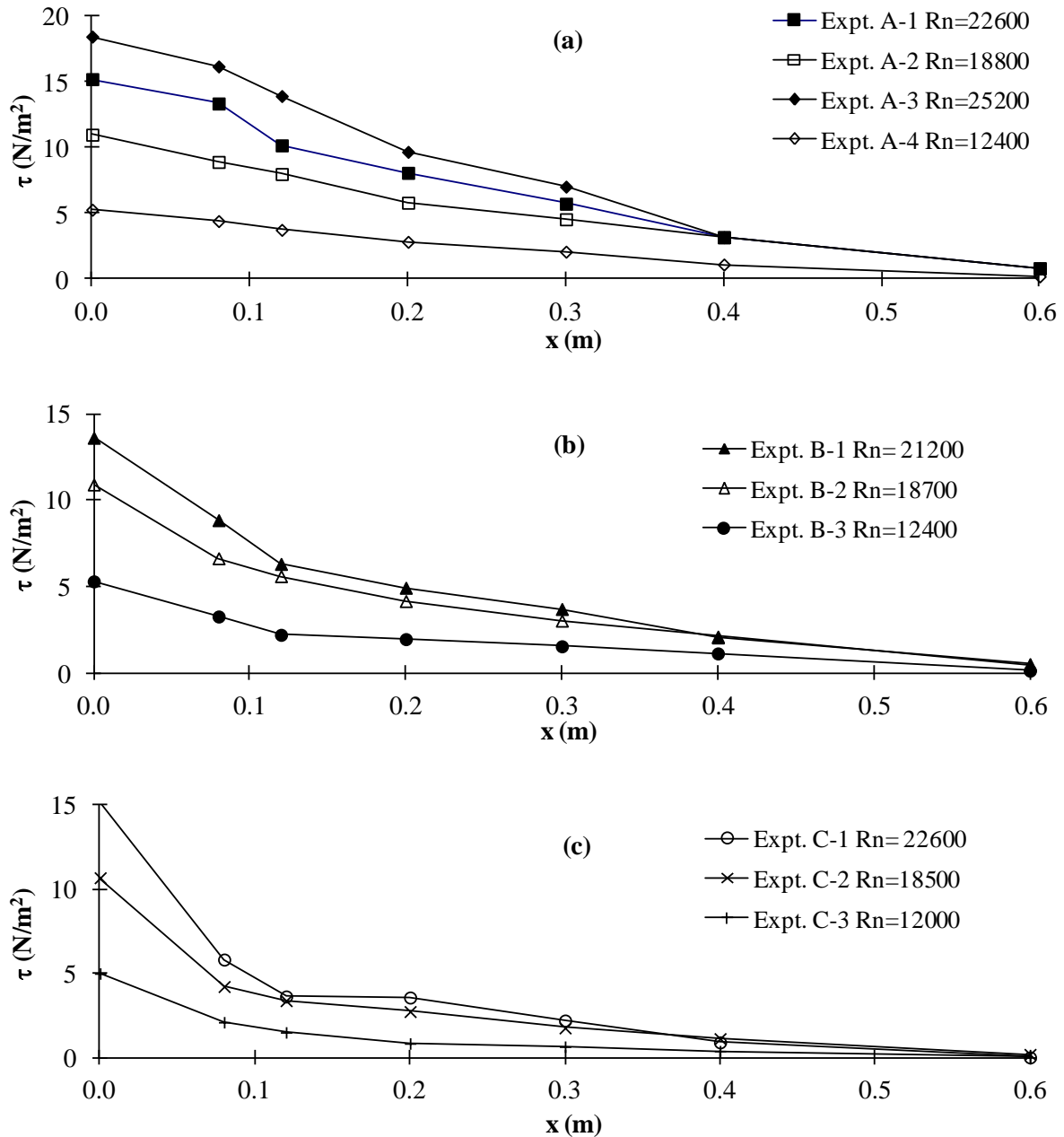


Fig. 12 The variation of the shear stress with the distance.
 (a) Series A, (b) Series B and (c) Series C

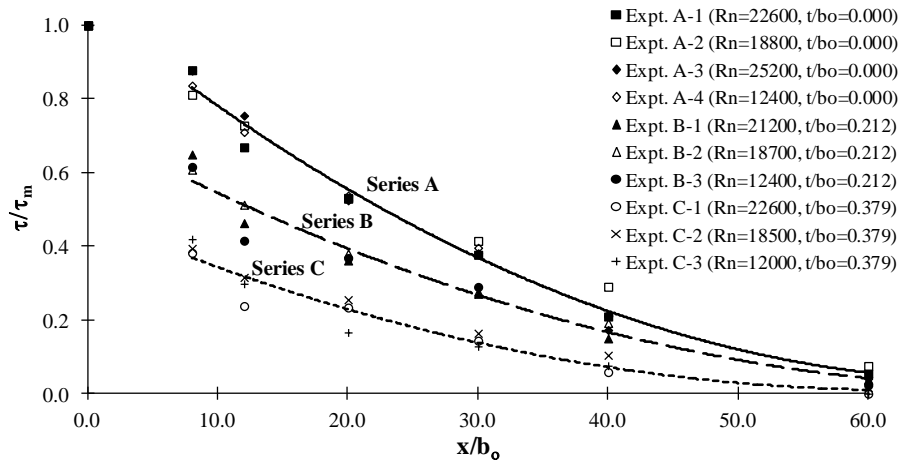


Fig. 13 Variation of the normalized shear stress, τ/τ_m with the normalized distance x/b_o

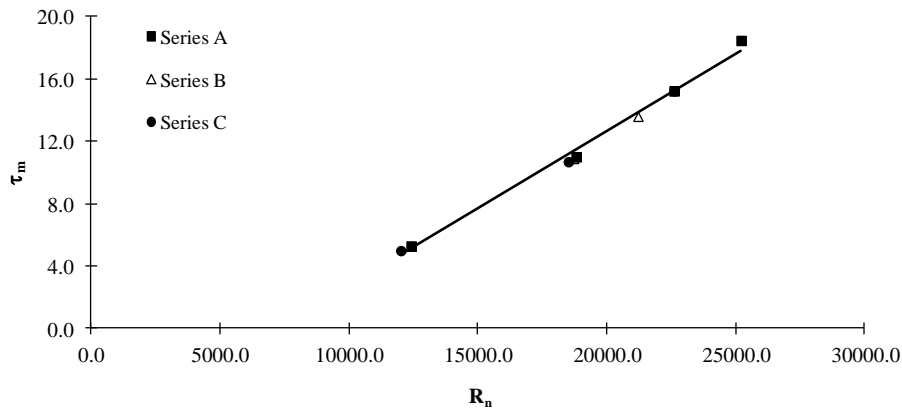


Fig. 14 The variation of the shear stress scale τ_m with R_n

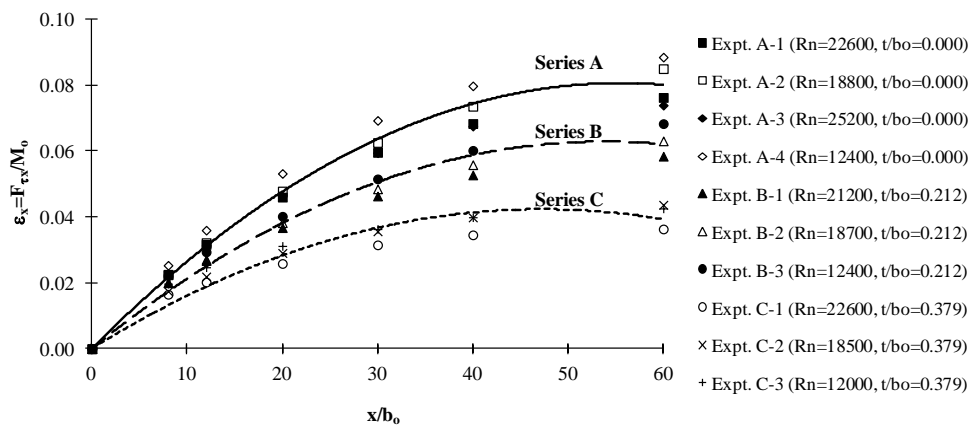


Fig. 15 Variation of the shear force coefficient ϵ_x with x/b_o

IV. Conclusions:

Based on an experimental study of plane turbulent wall jets on smooth and rough boundaries for a range of Froude numbers from 3.8 to 8.0 and for the depth ratio of 20, the following conclusions were drawn. The time averaged axial velocity profiles at x-stations along the longitudinal direction of the flume were similar. The velocity similarity profiles for wall jets in shallow tailwater deviated from those for the classical wall jet and this deviation increased with boundary roughness. The boundary layer thickness was also found to increase with boundary roughness. The length of the surface eddy decreased with the boundary roughness but increases with the Froude number. The decay of the maximum velocity occurred in two stages; in the first stage it

followed the decay of the maximum velocity for the classical wall jet and in the second stage the decay happened at a faster rate. Two stages were also observed in the growth of the jet half width with distance. The jet discharge, normalized with the discharge issuing from the slot, increased with the distance from the slot up to a certain section then it decreased to a value of 1. The jet momentum was not preserved, as it was previously assumed, it varied with distance in a similar manner to that of the jet discharge. An average loss of about 90% in the jet momentum was observed. The decay of the maximum velocity, the growth of the jet half width, the variation of the jet discharge and the jet momentum with distance were all found to be independent of the Froude number and the relative roughness. A depression in the water surface at the gate with respect to the tailwater depth was observed. This depression decreased with roughness and increased with the Froude number and this increase was more profound for rough boundaries than for smooth ones. The profiles of the shear stress normalized with the maximum shear stress were found to be similar for each series of experiments. The normalized shear stress decreased with the increase in relative roughness.

References:

- [1]. Albertson, M. L., Dai, Y. B., Jensen, R. A. & Rouse, H. (1950). "Diffusion of submerged jets." *Trans. ASCE*, 115, 639-697.
- [2]. Ead, S. A. (1999). "Plane Turbulent Jets in Shallow Tailwater and Their Application to Energy Dissipation." Ph.D. Thesis, University of Alberta.
- [3]. Ead, S. A. and Rajaratnam, N. (2002). "Plane Turbulent Wall Jets in Shallow Tailwater." *J. Eng. Mech.*, 128(2), pp. 143-155.
- [4]. Ead, S. A. and Rajaratnam, N. (2004). "Plane Turbulent Wall Jets on Rough boundaries with limited Tailwater." *J. Eng. Mech.*, 130(10), pp. 1245-1250.
- [5]. Förthmann, E. (1936). "Turbulent jet expansion." English translation NACA. TM- 789. (Original Paper in German, 1934. *Ing. Archiv.*, 5)
- [6]. Kishore, G., Dey, S. (2016). "Hydraulics of submerged offset-jets." *Hydraulic Structures and Water System Management*. 6th IAHR International Symposium on Hydraulic Structures, Portland, OR, 27-30 June (pp. 407-416).
- [7]. Kotsovinos, N. E. (1978). "A note on the conservation of the axial momentum of a turbulent jet." *J. Fluid Mech.*, 87(7), pp. 55-63.
- [8]. Patel, V. C. (1965). "Calibration of the Preston tube and limitations on its use in pressure gradients." *J. Fluid Mech.*, Vol.23, pp. 185-208.
- [9]. Preston, J. H. (1954). "The determination of turbulent skin friction by means of Pitot tubes." *J. Royal Aero. Soc.*, Vol. 54, pp. 109-121.
- [10]. Rajaratnam, N. (1976). *Turbulent Jets*. Elsevier Publishing Co, The Netherlands, 304p.
- [11]. Shabayek, S. A. (2007). "Submerged Jumps and Wall Jets." 18th Canadian Hydrotechnical Conference, Winnipeg, Manitoba, August 22-24, 2007.
- [12]. Shabayek, S. A. (2011). "Plane Turbulent Wall Jets in Limited Tailwater Depth" *International Journal of Engineering & Technology IJET-IJENS* Vol: 11 No: 06 pp 192-197.
- [13]. Wu, S. and Rajaratnam, N. (1995). "Effect of baffles on submerged flows" *J. Hydr. Engrg., ASCE*, 121(9), pp. 644-652.